Applied Energy 86 (2009) 1606–1616

Contents lists available at ScienceDirect

Applied Energy

journal homepage: www.elsevier.com/locate/apenergy

Control of thermally activated building systems (TABS) in intermittent operation with pulse width modulation

M. Gwerder [a,*], J. Tödtli [a], B. Lehmann [b], V. Dorer [b], W. Güntensperger [a], F. Renggli [a]

[a] Siemens Switzerland Inc., Building Technologies Group, Gubelstrasse 22, CH-6301 Zug, Switzerland
[b] Empa, Swiss Federal Laboratories for Materials Testing and Research, Laboratory for Building Technologies, Ueberlandstrasse 129, CH-8600 Duebendorf, Switzerland

ARTICLE INFO

Article history:
Received 22 August 2008
Received in revised form 9 January 2009
Accepted 10 January 2009
Available online 15 February 2009

Keywords:
Thermally activated building systems
Concrete core conditioning systems
Building control
Pulse width modulation
Intermittent operation

ABSTRACT

Thermally activated building systems (TABS) integrate the building structure as energy storage, and have proofed to be energy efficient and economic viable for the heating and cooling of buildings. Although TABS are increasingly used, in many cases control has remained an issue to be improved. In this paper, a method is outlined allowing for automated control of TABS in intermittent operation with pulse width modulation (PWM). This method represents one part of a TABS control solution with automatic switching between cooling and heating modes for variable comfort criteria which was published before. A first pulse width modulation control solution is derived based on a simple 1st order model of TABS. Then a second, even simpler solution is given that significantly reduces the tuning effort. Finally, the paper outlines a pulse width modulation control procedure and gives two application examples of the PWM control carried out in a laboratory test room.

1. Introduction

Thermally activated building systems (TABS) integrate the building structure as energy storage. They have emerged as an important element in the overall energy strategy of the building and have proofed to be an energy efficient and economical way for cooling and heating of buildings. Building elements such as structural floors and slabs provide either cooling by radiant and convective energy absorption from the space, or space heating by the release of stored energy. In contrast to radiant cooling by suspended ceiling panels, the dynamic thermal behavior of these elements is exploited. Such, peaks in energy demand are flattened and the actual cooling of the TABS elements can be shifted into night time, using the cold outside air for heat rejection [1–3].

Besides these advantages of TABS, however, the specification of control algorithms is difficult compared to conventional systems because of the thermal inertia of TABS. In particular, to comply with comfort requirements in different rooms with different gains within the same hydraulic zone may be challenging. Various control approaches have been implemented so far, but they often have disadvantages due to different control solutions for cooling and heating, too frequent switching between heating and cooling, the need for manual switching between heating and cooling mode, unnecessary high energy consumption for water circulation as well as the need for manual adjustment of parameters.

Therefore the objective was to develop control algorithms for year-round automated operation of TABS, which meet the comfort requirements, at the same time are simple to commission and lead to an energy efficient operation.

This paper explicitly presents one part – the intermittent operation with pulse width modulation (PWM) control – of a newly developed, comprehensive strategy for the temperature control of rooms with TABS, considering the prediction uncertainty of heat gains during operation by specifying respective bounds. The strategy has been developed in the frame of a research project on which was reported the first time in [4] and which is described in more detail in [5]. Section 2 outlines control concepts for TABS and the modules of the new control concept including the PWM module. Section 3 describes the thermal model used for PWM control. Section 4 outlines the PWM control method developed using and comparing two different calculation approaches. Section 5 demonstrates the applicability and performance of the PWM control methods based on results from a detailed building simulation and evaluations in laboratory tests.

In this paper, PWM control methods and their integration into TABS zone control are presented in detail. The design of TABS and the control functionality besides PWM control as well as the comparison between different control in terms of energy consumption and comfort are not subject of this paper. These topics are addressed in separate publications.

* Corresponding author. Tel.: +41 41 724 40 27; fax: +41 41 723 54 06.
E-mail address: markus.gwerder@siemens.com (M. Gwerder).

0306-2619/$ - see front matter © 2009 Elsevier Ltd. All rights reserved.
doi:10.1016/j.apenergy.2009.01.008

Nomenclature

C	capacitance, J/K
CC	cooling curve, –
E	energy, J
HC	heating curve, –
$\dot{q}$	heat flux, W/m^2
R	thermal resistance, m^2 K/W
R_t	thermal resistance piping system TABS, m^2 K/W
$\tilde{R}$	thermal resistance between core and room temperature, m^2 K/W
$R_{l,f}$	thermal resistance façade, in relation to floor area, m^2 K/W
T	time, s or h

Greek symbols

Δ	difference
ϑ	temperature, °C
τ	time constant, s or h

Subscripts

0,1	zone pump off/on
1,2	zone number
c	core
C	cooling
cont	continuous
elb	equivalent lower bound
eub	equivalent upper bound
FB	feedback (room temperature)
g	gain
H	heating
l,f	loss façade
Min	minimal
Max	maximal
oa	outside air, weather zone air
p	pipe
Purge	purge
PWM	pulse width modulation
r	room
rw	return water
s	slab
Sp	set-point
SpC,SpH,SpU	set-point cooling/heating/undefined
sw	supply water
t	total
U	undefined
w	water
x,z	coordinates, directions

2. Control concepts for TABS

2.1. Conventional control concepts for TABS

So far, only a few authors have reported on control of TABS, including Meierhans as one of the TABS pioneers [6], Olesen [7], Antonopoulos et al. [8] and Weitzmann [9] with a short overview. Tödtli et al. [4] evaluated existing control solutions and concluded that they mostly have the following properties: (a) they are based on an outside temperature compensated supply water temperature control, the set-point of the supply water temperature being shifted with varying outside temperature according to the heating curve without considering heat gains, and the cooling curve typically being a constant supply water temperature set-point based on the maximum load situation. (b) No feed-back variable from the zones (return temperature, concrete core temperature or room temperature) is used for the control, thus banking on the self-regulation effects of the concrete core conditioning system. (c) The heat and cold generation are enabled or activated dependant on the season and/or the outside temperature. (d) Free cooling is accounted for in a heuristic way.

2.2. New control concept

In [5,10], a new control concept was presented that is one part of an integrated process consisting of the tasks to design a TABS (planning of HVAC system and of its control [11]), to commission it and to optimize it during operation [12]. In the design phase of a TABS, a base TABS zone control strategy is selected that only reflects the basic control action, e.g. the base control strategy "supply water temperature control" (see Figs. 1 and 2, control with mandatory parts only). In real operation, this base control strategy can be extended by optional control parts to improve comfort and/or energy efficiency depending on given requirements and installations [10] (see Fig. 2, optional control parts). The result is a modular control concept for a TABS zone which – by configuration – can be adapted to different TABS plants. Besides the zones, also the heat and cold generation and distribution have to be controlled. In this paper only the TABS zone control and in particular the intermittent operation of the zone pumps is described in detail.

In Fig. 1, the overall control concept for a TABS plant with two zones is shown. Both zone controllers are fed with the following signals: outside air temperature ϑ_{oa}, supply water temperature ϑ_{sw}, room temperature ϑ_r (optional) and room temperature set-point range $[\vartheta_{r,SpH}, \vartheta_{r,SpC}]$. The zone controllers operate the zone pumps (on/off) and the zone heating and cooling valves. Together with the zone supply water temperature set-points $\vartheta_{sw,SpH,PWM}$ and $\vartheta_{sw,SpC,PWM}$, these signals can also be used to set up a demand dependent control of the heat and cold generation and distribution as indicated in Fig. 1.

In Fig. 2, the TABS zone control is shown in more detail. The control is modular, i.e. it contains two or more functionality parts. Mandatory parts are indicated by solid frames, optional parts by dotted frames. If an optional part is not needed or required, only the feed-through indicated by dotted arrows in the corresponding control part function block has to be realized. The functionalities of the four control parts are explained below.

2.2.1. Room temperature feedback control

If one or several room temperatures ϑ_r are measured in the controlled zone, a room temperature feedback control part can be added to the zone control. Since TABS react slowly, only day-to-day room temperature compensation is promising, an instant correction can not be achieved with TABS. In Fig. 2, the room temperature controller adjusts the desired room temperature set-point range $[\vartheta_{r,SpH}, \vartheta_{r,SpC}]$ to a corrected set-point range $[\vartheta_{r,SpH,FB}, \vartheta_{r,SpC,FB}]$ that is processed in the further control parts in order to maintain the room temperature within $[\vartheta_{r,SpH}, \vartheta_{r,SpC}]$. Advantages and disadvantages of room temperature control as well as a realization example are given in [10].

2.2.2. Outside air temperature compensated supply water temperature control

This core control part determines a supply water temperature set-point range $[\vartheta_{sw,SpH}, \vartheta_{sw,SpC}]$ as a function of the mean outside air temperature $\overline{\vartheta}_{oa}$ of the last 24 h (moving time window) and

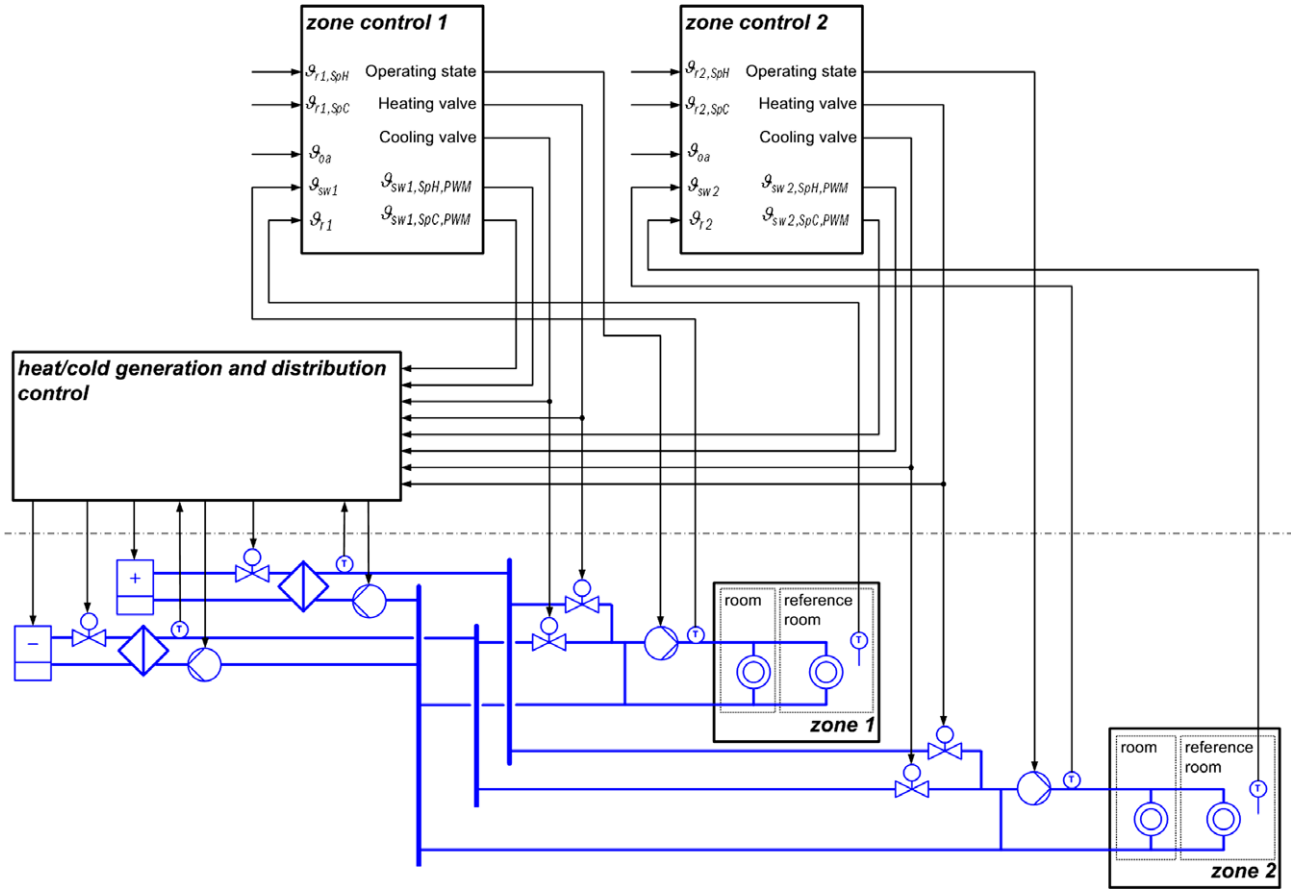

Fig. 1. The overall TABS control concept, including heat/cold generation and distribution system.

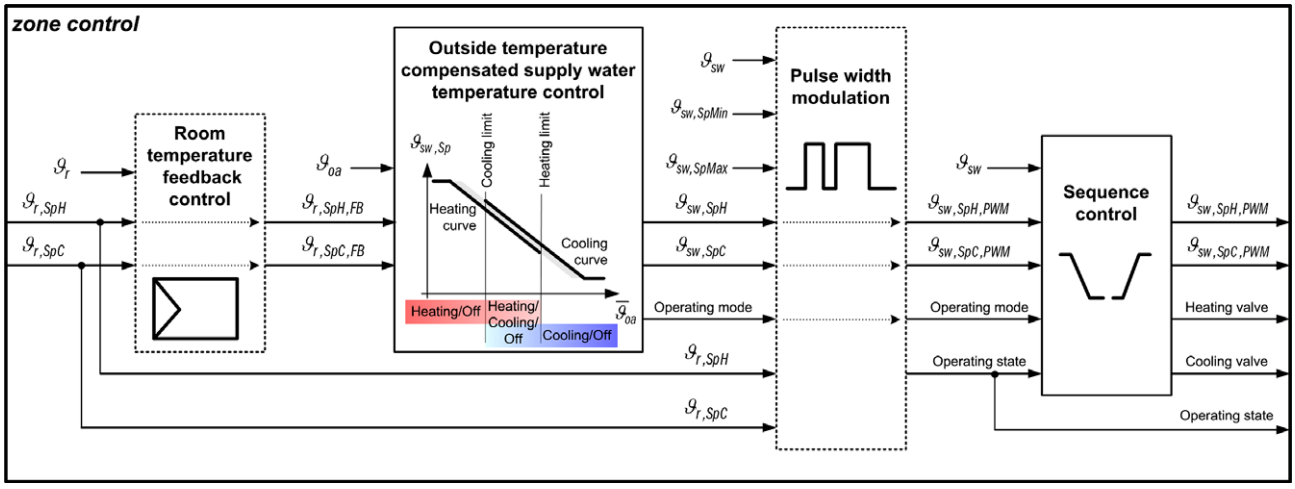

Fig. 2. Scheme of the modular zone control (mandatory parts with solid frame, optional parts with dotted frame).

the current room temperature set-point range $[\vartheta_{r,SpH,FB}, \vartheta_{r,SpC,FB}]$. For that purpose, the so called heating curve (HC) and cooling curve (CC) are used. The heating and cooling limits serve to identify the operating mode depending on $\overline{\vartheta}_{oa}$ (see Fig. 2). In order to define initial parameters of this control part, an unknown-but-bounded design process can be followed [5,11]. Detailed information on this control part and its application can be found in [12].

2.2.3. Pulse width modulation

The control parts presented so far are based on continuous operation of the zone pumps. A third control part (see Fig. 2) can be added to operate the zone water circulation pump in intermittent operation with pulse width modulation (PWM). Advantages and disadvantages of intermittent operation control are given in [10].

2.2.4. Sequence control

A standard sequence controller that controls the supply water temperature ϑ_{sw} (the according set-point range is $[\vartheta_{sw,SpH,PWM}, \vartheta_{sw,SpC,PWM}]$) is acting on the heating and cooling valves. Depending on operating mode and operating state (i.e. pump on/off command) one or both sequences are disabled and the respective valve is closed.

3. A simple thermal model for TABS

The PWM control method introduced in Section 2.2 is derived from a simple dynamic thermal model that reflects the thermal behavior of TABS. Therefore, this model is described first, followed by the detailed derivation of the PWM control method.

3.1. Modeling of the piping system

For the purposes of design and performance simulations of TABS, a model was developed which depicts the heat transfer in the slab and to adjacent rooms [3]. This TABS model – under certain restrictions – allows reducing the 3-dim heat transfer in the slab to a 1-dim approach by establishing a correlation between supply water temperature, core temperature (mean slab temperature in the plane of the piping system) and room temperature (operative temperature). The main parameter to model the piping system is the equivalent resistance R_t, in which the geometrical characteristic, material parameters and the influence of the fluid mass flow are summarized (Fig. 3). The dynamic thermal behavior of the upper and lower parts of the slab can be modeled in an arbitrarily complex manner ranging from a simple 1-node-model as used in this paper (see Section 3.2) to detailed multi-layer models. A detailed description of the TABS-resistances can be found either in [5] (Appendix 1) or [13] (Annex B).

3.2. Dynamic thermal model of TABS room

As thermal inertia plays a pivotal role in the behavior of TABS, a model used for TABS pulse width modulation should reflect in particular the thermal behavior of the activated thermal mass. Fig. 4 shows the structure of a 1st-order resistance–capacitance model. The slab core temperature node ϑ_c with thermal capacitance C_s is linked to the supply water temperature ϑ_{sw} by the TABS-resistance R_t (only if zone pump is running) and to the operative room temperature ϑ_r by the resistance $\tilde{R}$. The internal and solar heat gains $\dot{q}_g$ affect the room node which is linked to the outside air temperature ϑ_{oa} by a façade-resistance $R_{l,f}$ (calculation of resistances see [3] or [5]).

The 1st-order differential equation for the slab core temperature node of the model with running zone pump can be written:

$$C_s\left(\frac{R_t(\tilde{R}+R_{l,f})}{R_t+\tilde{R}+R_{l,f}}\right)\frac{d\vartheta_c(t)}{dt} = -\vartheta_c(t) + \frac{\tilde{R}+R_{l,f}}{R_t+\tilde{R}+R_{l,f}}\vartheta_{sw}(t) + \frac{R_t}{R_t+\tilde{R}+R_{l,f}}(\vartheta_{oa}(t)+R_{l,f}\dot{q}_g(t)) \quad (1)$$

We substitute two terms: the time constant of the model τ_1 and the perturbation $\vartheta_{c1}(t)$.

$$\tau_1 = C_s\left(\frac{R_t(\tilde{R}+R_{l,f})}{R_t+\tilde{R}+R_{l,f}}\right) \quad (2)$$

$$\vartheta_{c1}(t) = \frac{\tilde{R}+R_{l,f}}{R_t+\tilde{R}+R_{l,f}}\vartheta_{sw}(t) + \frac{R_t}{R_t+\tilde{R}+R_{l,f}}(\vartheta_{oa}(t)+R_{l,f}\dot{q}_g(t)) \quad (3)$$

For constant $\vartheta_{oa}, \vartheta_{sw}$ and $\dot{q}_g$, the solution of (1) is given by (4). The stationary solution is then given by ϑ_{c1}.

$$\vartheta_c(t) = \vartheta_{c1} + (\vartheta_c(0) - \vartheta_{c1})\cdot e^{-\frac{t}{\tau_1}} \quad (4)$$

The first order differential equation for the slab core temperature node of the model with zone pump deactivated can be written:

$$C_s(\tilde{R}+R_{l,f})\frac{d\vartheta_c(t)}{dt} = -\vartheta_c(t) + \vartheta_{oa}(t) + R_{l,f}\dot{q}_g(t) \quad (5)$$

Again, we substitute two terms: the time constant of the model τ_0 and the perturbation $\vartheta_{c0}(t)$:

$$\tau_0 = C_s(\tilde{R}+R_{l,f}) \quad (6)$$

$$\vartheta_{c0}(t) = \vartheta_{oa}(t) + R_{l,f}\dot{q}_g(t) \quad (7)$$

For constant ϑ_{oa} and $\dot{q}_g$, the solution of (5) is given by (8). The stationary solution is then given by ϑ_{c0}.

$$\vartheta_c(t) = \vartheta_{c0} + (\vartheta_c(0) - \vartheta_{c0})\cdot e^{-\frac{t}{\tau_0}} \quad (8)$$

4. Pulse width modulation (PWM) control

4.1. PWM calculations using 1st order model

Here, the 1st order model from Section 3.2 is taken for PWM calculations. A similar calculation procedure for a different application can be found in [14].

Firstly, we examine the heating mode where heat is delivered to the thermally activated structure. In order to maintain a room temperature ϑ_r which is equal or higher than the lower room temperature set-point $\vartheta_{r,SpH}$ also the core temperature must be kept above

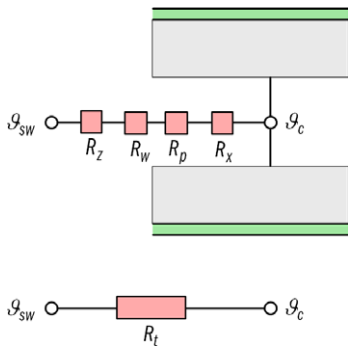

Fig. 3. Piping system embedded in a slab and corresponding model representation.

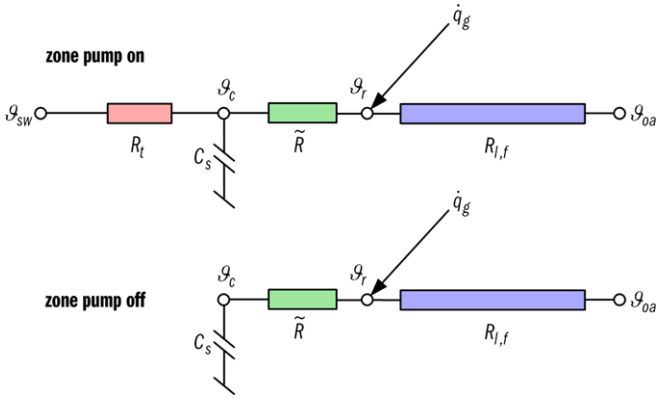

Fig. 4. Resistance–capacitance model of the room for zone pump switched on (above) and zone pump switched off (below).

a certain level. This minimal core temperature $\vartheta_{c,Min}$ can be calculated as (see Fig. 4):

$$\vartheta_{c,Min} = \vartheta_{r,SpH} + \frac{\tilde{R}}{R_{l,f}}(\vartheta_{r,SpH} - \vartheta_{oa}) - \tilde{R}\dot{q}_g \tag{9}$$

Considering a quasi-stationary operation with constant ϑ_{oa}, constant $\vartheta_{sw} = \vartheta_{sw,SpH,PWM}$, constant $\dot{q}_g = \dot{q}_{g,elb}$ and the zone pump switching on and off with constant switched-on phase Δt_1 and constant switched-off phase Δt_0, the core temperature has always to be equal or higher than $\vartheta_{c,Min}$. As can be seen from (10) at the beginning of a new switched-on phase (time $\Delta t_1 + \Delta t_0$) the core temperature ϑ_c has to be equal to $\vartheta_{c,Min}$.

$$\begin{aligned}\vartheta_c(\Delta t_1) &= \vartheta_{c1} + (\vartheta_{c,Min} - \vartheta_{c1}) \cdot e^{-\frac{\Delta t_1}{\tau_1}} \\ \vartheta_c(\Delta t_1 + \Delta t_0) &= \vartheta_{c0} + (\vartheta_c(\Delta t_1) - \vartheta_{c0}) \cdot e^{-\frac{\Delta t_0}{\tau_0}} = \vartheta_{c0} \\ &\quad + (\vartheta_{c1} + (\vartheta_{c,Min} - \vartheta_{c1})e^{-\frac{\Delta t_1}{\tau_1}} - \vartheta_{c0}) \cdot e^{-\frac{\Delta t_0}{\tau_0}} = \vartheta_{c,Min}\end{aligned} \tag{10}$$

Combining (3), (7), and (10), the correlation (11) describing the PWM operation is obtained:

$$\begin{aligned}\vartheta_{c,Min} = \vartheta_{c0} &+ \left(\frac{\tilde{R} + R_{l,f}}{R_t + \tilde{R} + R_{l,f}}(\vartheta_{sw,SpH,PWM} - \vartheta_{c0})\right. \\ &\left. + \left(\vartheta_{c,Min} - \frac{\tilde{R} + R_{l,f}}{R_t + \tilde{R} + R_{l,f}}\vartheta_{sw,SpH,PWM} - \frac{R_t}{R_t + \tilde{R} + R_{l,f}}\vartheta_{c0}\right) \cdot e^{-\frac{\Delta t_1}{\tau_1}}\right) \cdot e^{-\frac{\Delta t_0}{\tau_0}}\end{aligned} \tag{11}$$

Depending on what type of PWM control is desired, two out of the three quantities $\vartheta_{sw,SpH,PWM}$, Δt_0 and Δt_1 can be defined and the third one then can be calculated by applying (11). Doing so for given Δt_0 and Δt_1, we obtain (12) for $\vartheta_{sw,SpH,PWM}$ in the heating mode.

$$\begin{aligned}\vartheta_{sw,SpH,PWM} = &\frac{R_t + \tilde{R} + R_{l,f}}{\tilde{R} + R_{l,f}} \\ &\times \left[\frac{\vartheta_{c,Min}\left(1 - e^{-\frac{\Delta t_0}{\tau_0}e^{-\frac{\Delta t_1}{\tau_1}}}\right) - \vartheta_{c0}\left(1 - e^{-\frac{\Delta t_0}{\tau_0}}\right)}{e^{-\frac{\Delta t_0}{\tau_0}}\left(1 - e^{-\frac{\Delta t_1}{\tau_1}}\right)} - \frac{R_t}{R_t + \tilde{R} + R_{l,f}}\vartheta_{c0}\right]\end{aligned} \tag{12}$$

When following a similar procedure for the cooling mode, a corresponding result can be derived. There a maximum core temperature $\vartheta_{c,Max}$ can be calculated (see Fig. 4) in order to maintain a room temperature which is equal or lower than the upper room temperature set-point $\vartheta_{r,SpC}$:

$$\vartheta_{c,Max} = \vartheta_{r,SpC} + \frac{\tilde{R}}{R_{l,f}}(\vartheta_{r,SpC} - \vartheta_{oa}) - \tilde{R}\dot{q}_g \tag{13}$$

By treating a quasi-stationary operation (constant switched-on phase Δt_1 and constant switched-off phase Δt_0, constant ϑ_{oa}, constant $\vartheta_{sw} = \vartheta_{sw,SpC,PWM}$ and constant $\dot{q}_g = \dot{q}_{g,eub}$), we obtain a result similar to (12) for the cooling mode:

$$\begin{aligned}\vartheta_{sw,SpC,PWM} = &\frac{R_t + \tilde{R} + R_{l,f}}{\tilde{R} + R_{l,f}} \\ &\times \left[\frac{\vartheta_{c,Max}\left(1 - e^{-\frac{\Delta t_0}{\tau_0}e^{-\frac{\Delta t_1}{\tau_1}}}\right) - \vartheta_{c0}\left(1 - e^{-\frac{\Delta t_0}{\tau_0}}\right)}{e^{-\frac{\Delta t_0}{\tau_0}}\left(1 - e^{-\frac{\Delta t_1}{\tau_1}}\right)} - \frac{R_t}{R_t + \tilde{R} + R_{l,f}}\vartheta_{c0}\right]\end{aligned} \tag{14}$$

The deduced Eqs. (12) and (14) are perfectly valid only for ideal quasi-stationary operation with constant disturbances. Since in these equations, *equivalent* heat gain bounds are used that are constant for at least 24 h (see [5]), the equations can also be used for non-constant heat gains as can be seen in Section 5.3. For the outside air temperature disturbance, not the actual value is taken but instead a typically very slowly moving average of the last 24 h (moving time window), see Section 2.2. By considering these measures, the altered disturbances are approximately constant during the PWM period and the use of Eqs. (12) and (14) in such a way is adequate also in non-ideal operation as has been shown by simulations [12].

4.2. Simplified PWM calculations

As an alternative to the method using a 1st order model, a second approach for PWM calculation is derived here which is solely based on an energy contemplation. The basic idea of this second approach is that during the switch-on phase with PWM operation an equal amount of energy has to be delivered to the thermally activated structure as would have been delivered during the time span of an entire PWM cycle but with continuous pump operation. Again, we consider first the heating mode where $\vartheta_c \geqslant \vartheta_{c,Min}$ is required in order to maintain thermal comfort in the room.

In continuous operation, the energy input E_{cont} over one PWM period Δt_H for constant ϑ_{oa}, constant $\vartheta_{sw} = \vartheta_{sw,SpH}$ and constant $\dot{q}_g = \dot{q}_{g,elb}$ is given by

$$\begin{aligned}E_{cont} &= \frac{1}{R_t}\int_{t=0}^{\Delta t_H}(\vartheta_{sw,SpH} - \vartheta_{c,Min})dt = \frac{\Delta t_H}{R_t}(\vartheta_{sw,SpH} - \vartheta_{c,Min}) \\ &= \frac{\Delta t_H}{R_t + \tilde{R}}(\vartheta_{sw,SpH} - \vartheta_{r,SpH})\end{aligned} \tag{15}$$

In intermittent operation, the energy input E_{PWM} over one PWM period Δt_H for constant ϑ_{oa}, constant $\vartheta_{sw} = \vartheta_{sw,SpH,PWM}$ and constant $\dot{q}_g = \dot{q}_{g,elb}$ can be calculated in a similar way. Since in PWM operation, the pump is only partially running, the integration over time only runs from pump switch-on to switch-off time, i.e. from 0 to $\Delta t_{1,H}$:

$$\begin{aligned}E_{PWM} &= \frac{1}{R_t}\int_{t=0}^{\Delta t_{1,H}}(\vartheta_{sw,SpH,PWM} - \vartheta_c(t))dt \\ &= \frac{1}{R_t}\int_{t=0}^{\Delta t_{1,H}}\left(\vartheta_{sw,SpH,PWM} - \left[\vartheta_{c1} + (\vartheta_{c,Min} - \vartheta_{c1}) \cdot e^{-\frac{t}{\tau_1}}\right]\right)dt \\ &= \frac{\Delta t_{1,H}}{R_t}(\vartheta_{sw,SpH,PWM} - \vartheta_{c1}) - \frac{\tau_1}{R_t}(\vartheta_{c1} - \vartheta_{c,Min}) \\ &\quad \cdot \left(e^{-\frac{\Delta t_{1,H}}{\tau_1}} - 1\right)\end{aligned} \tag{16}$$

In (16), the core temperature is taken from (4). For $\Delta t_{1,H}/\tau_1 << 1$, the approximation $e^{-\Delta t_{1,H}/\tau_1} \approx 1 - \Delta t_{1,H}/\tau_1$ can be used. By incorporating this approximation in (16) E_{PWM} is derived as

$$E_{PWM} = \frac{\Delta t_{1,H}}{R_t}(\vartheta_{sw,SpH,PWM} - \vartheta_{c,Min}) \tag{17}$$

As will be shown later this leads to a much simpler PWM control solution.

When postulating that in both operating scenarios – PWM and continuous operation – the same amount of heating energy has to be delivered to the thermally activated structure ($E_{PWM} = E_{cont}$), we obtain:

$$\frac{\Delta t_{1,H}}{\Delta t_H} = \frac{\vartheta_{sw,SpH} - \vartheta_{c,Min}}{\vartheta_{sw,SpH,PWM} - \vartheta_{c,Min}} \tag{18}$$

By using (15), an expression for $\vartheta_{c,Min}$ can be found:

$$\vartheta_{c,Min} = \vartheta_{sw,SpH} - \frac{R_t}{R_t + \tilde{R}}(\vartheta_{sw,SpH} - \vartheta_{r,SpH}) \tag{19}$$

Finally, by combining (18) and (19), we receive a PWM control solution for the ratio between the switched-on phase $\Delta t_{1,H}$ and the period Δt_H for given lower room temperature set-point $\vartheta_{r,SpH}$, continuous operation supply water temperature set-point $\vartheta_{sw,SpH}$ and (to be applied) PWM supply water temperature set-point $\vartheta_{sw,SpH,PWM}$:

$$\frac{\Delta t_{1,H}}{\Delta t_H} = \frac{1}{1 + \frac{\vartheta_{sw,SpH,PWM} - \vartheta_{sw,SpH}}{\frac{R_t}{R_t+\tilde{R}} \cdot (\vartheta_{sw,SpH} - \vartheta_{r,SpH})}} \tag{20}$$

Again, as in (11), two out of the three quantities $\vartheta_{sw,SpH,PWM}$, Δt_H and $\Delta t_{1,H}$ can be defined and the third one then can be calculated by applying (20) depending on what type of PWM control is desired (see also (26)). A similar result to (20) can be found for the cooling mode:

$$\frac{\Delta t_{1,C}}{\Delta t_C} = \frac{1}{1 + \frac{\vartheta_{sw,SpC} - \vartheta_{sw,SpC,PWM}}{\frac{R_t}{R_t+\tilde{R}} \cdot (\vartheta_{r,SpC} - \vartheta_{sw,SpC})}} \tag{21}$$

If it is not clear whether heating or cooling is required, there still exists a PWM solution. In this so-called PWM mode *undefined* (cf. Fig. 7), the supply water temperature set-point range $[\vartheta_{sw,SpH}, \vartheta_{sw,SpC}]$ can be reduced to a specified width $\Delta\vartheta_{sw,SpU,PWM}$ (possible if $\Delta\vartheta_{sw,SpU,PWM} < \vartheta_{sw,SpC} - \vartheta_{sw,SpH}$). When calculating $\Delta\vartheta_{sw,SpU,PWM}$ by using (20) and (21) and setting $\Delta t_{1,H} = \Delta t_{1,C} = \Delta t_{1,U}$ and $\Delta t_H = \Delta t_C = \Delta t_U$, we get a result similar to (20) and (21) for the undefined mode:

$$\frac{\Delta t_{1,U}}{\Delta t_U} = \frac{1}{1 + \frac{\Delta\vartheta_{sw,Sp} - \Delta\vartheta_{sw,SpU,PWM}}{\frac{R_t}{R_t+\tilde{R}} \cdot (\Delta\vartheta_{r,Sp} - \Delta\vartheta_{sw,Sp})}} \tag{22}$$

In (20)–(22), it can be seen that the only appearing physical PWM parameter is the thermal resistance ratio $R_t/(R_t + \tilde{R})$ which allows for easy tuning compared to the PWM solution of Section 4.1. The remaining PWM control parameters are the room temperature set-points $\vartheta_{r,SpH}$, $\vartheta_{r,SpC}$ (also needed in other control), the supply water temperature set-points for PWM operation $\vartheta_{sw,SpH,PWM}$, $\vartheta_{sw,SpC,PWM}$, $\Delta\vartheta_{sw,SpU,PWM}$ and the PWM operation parameters Δt_H, Δt_C, and Δt_U.

In Fig. 5, thermal resistance ratios $R_t/(R_t + \tilde{R})$ are shown dependent on the thermal resistances R_t and $\tilde{R}$ together with typical ranges of these resistances for TABS. Typical thermal resistance ratios $R_t/(R_t + \tilde{R})$ are in the range of 20–50%. Values for R_t mainly increase with wider TABS pipe spacing and lower water mass flow rate, values for $\tilde{R}$ increase primarily for floor and ceiling coverings with higher thermal resistances.

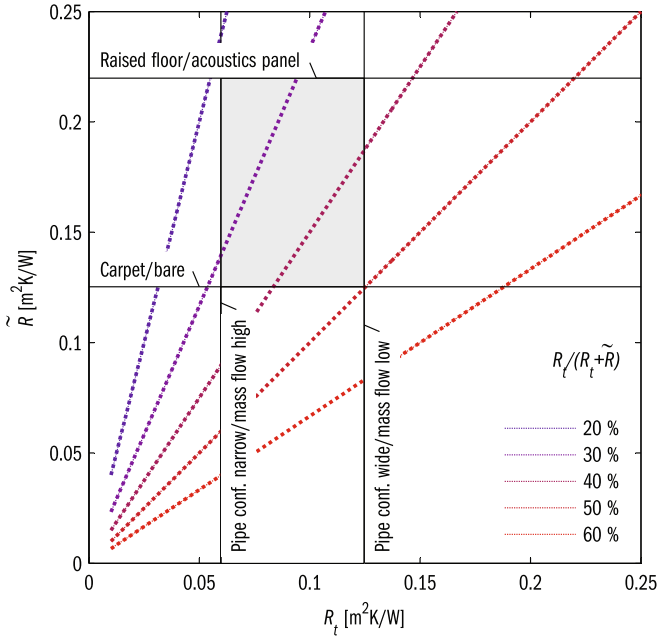

Fig. 5. Thermal resistances for different TABS configurations and resulting thermal resistance ratio $R_t/(R_t + \tilde{R})$. The grayed out area marks the typical range of thermal resistances for TABS.

4.3. Comparison of PWM calculations

In Fig. 6 the pump switched-on phases calculated using PWM control solutions based on the 1st order model calculations (Section 4.1) and based on the simplified calculations (Section 4.2) are compared. The parameters and data used for the PWM calculations are given in Table 1. The values are deduced from the labora-

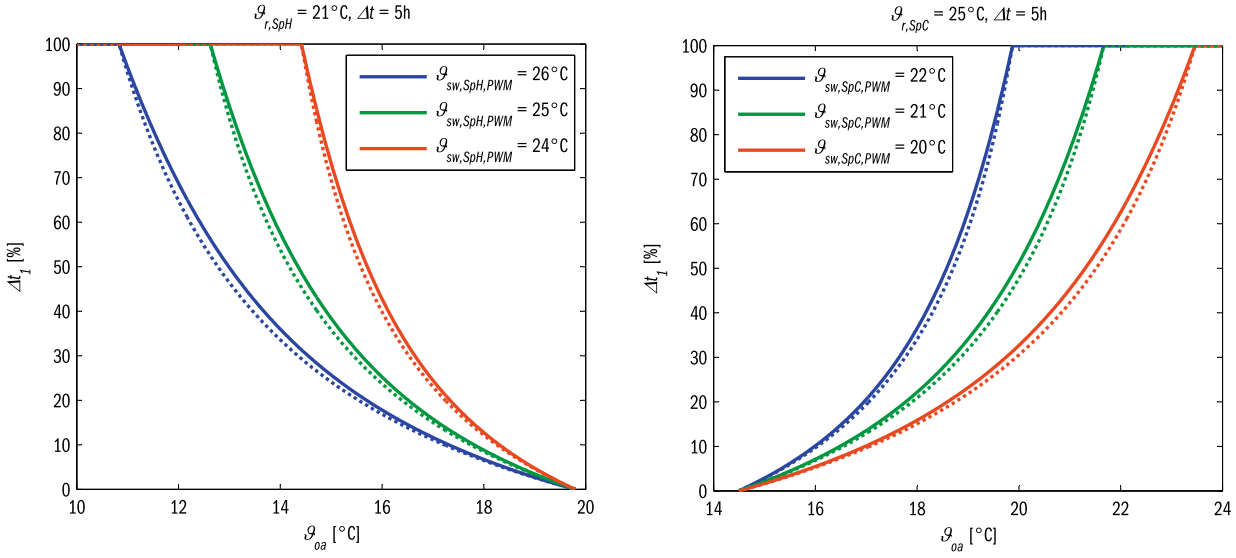

Fig. 6. Comparison of pump switched-on phases for PWM control solutions based on 1st order model calculations (solid lines) and based on simplified calculations (dotted lines).

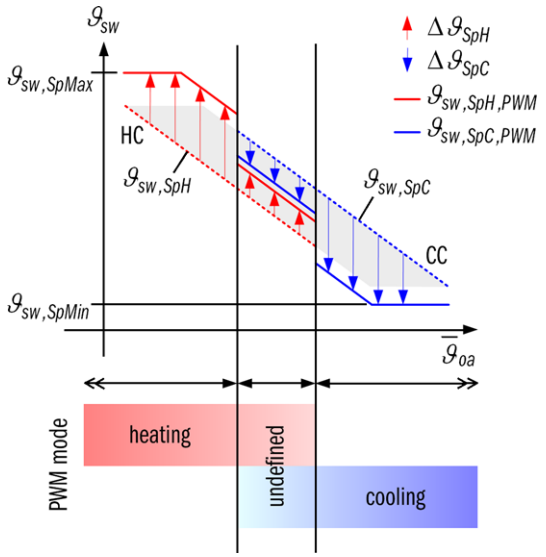

Fig. 7. PWM mode and supply water temperature set-points depending on the mean outside air temperature $\overline{\vartheta}_{oa}$.

Table 1
Parameters and data for the PWM calculations deduced from the laboratory set-up.

Thermal resistances	m^2 K/W
R_t	0.060
$\tilde{R}$	0.16
$R_{t,f}$	0.39
Time constants	**h**
τ_1	9.9
τ_0	100
Equivalent lower and upper bound heat gains	**W/m^2**
$\dot{q}_{g,elb}$ (heating mode)	3.1
$\dot{q}_{g,eub}$ (cooling mode)	27

tory set-up analyzed in Section 5. The thermal resistances of Table 1 yield a thermal resistance ratio $R_t/(R_t+\tilde{R})$ of 28%.

A PWM period Δt of 5 h, a lower room temperature set-point $\vartheta_{r,SpH}$ of 21 °C and an upper room temperature set-point $\vartheta_{r,SpC}$ of 25 °C were used to generate Fig. 6. Results for three different supply water temperature set-points are given.

In the example presented here, the difference of the two models in terms of relative pump switched-on phases is small. In this case the simplified PWM calculations are sufficiently accurate. Investigations show that for typical core-activated building structures, periods Δt up to 24 h can be treated with simplified PWM calculations.

4.4. Non-constant supply water temperatures during pump switched-on phases

So far, we assumed that the supply water temperature ϑ_{sw} was equal to the according set-point $\vartheta_{sw,SpH,PWM}$ (or $\vartheta_{sw,SpC,PWM}$, respectively) during the pump switched-on phases. In reality, there are several reasons why ϑ_{sw} will differ from its set-point:

- Non-ideal supply water temperature control caused by disturbances or bad tuning of the supply water temperature controller.
- Limitation or special features of heat or cold generation, e.g. when using cooling tower(s) for cooling exclusively.

Because of these reasons, a PWM solution that is able to cope with non-constant supply water temperatures is desirable. Starting with Eq. (16), we can derive such a solution based on the assumption that the core temperature (ϑ_c) devolution is equal to the case with constant supply water temperature ϑ_{sw}:

$$\frac{\Delta t_1}{\Delta t} = \frac{\frac{1}{\Delta t}\int_{t=0}^{\Delta t_1}\vartheta_{sw}(t)dt - \frac{R_t}{R_t+\tilde{R}}\cdot(\vartheta_{sw,Sp}-\vartheta_{r,Sp})}{\vartheta_{sw,Sp}-\frac{R_t}{R_t+\tilde{R}}\cdot(\vartheta_{sw,Sp}-\vartheta_{r,Sp})} \tag{23}$$

Eq. (23) can be applied in the heating, cooling and the undefined mode. In reality, the assumptions made will not be met perfectly, but – as simulation studies show – (23) can be applied in all typical cases.

4.5. Implementation of PWM in zone control

In this Section, the basic functionality of the control module "Pulse width modulation" in Fig. 2 is explained for the simplified PWM calculations. Depending on the operating mode of the module "Outside air temperature compensated supply water temperature control", the PWM module operates either in *heating* mode, *cooling* mode, *undefined* mode or *off* mode (PWM mode, see Fig. 7, cf. Fig. 2). Fig. 7 also shows suggested supply water temperature set-points $\vartheta_{sw,SpH,PWM}$ and $\vartheta_{sw,SpC,PWM}$ for the different PWM modes. In the following, the real-time calculation procedure performed in the PWM module is outlined in two steps.

4.5.1. Determine supply water temperature set-points

At the beginning of each PWM period Δt, the PWM mode is determined and kept for the whole period. In the *heating* mode, the PWM supply water temperature set-point $\vartheta_{sw,SpH,PWM}$ has to be calculated. For this purpose, the supply water temperature for continuous operation $\vartheta_{sw,SpH}$ is shifted by $\Delta\vartheta_{SpH}$. In order not to reduce the self-regulation of TABS substantially, $\Delta\vartheta_{SpH}$ should be relatively small (typically $\Delta\vartheta_{SpH}$ is in the range of 1–3 K). In addition $\vartheta_{sw,SpH,PWM}$ is limited to a maximal set-point $\vartheta_{sw,SpMax}$ (see Fig. 7).

$$\vartheta_{sw,SpH,PWM} = \min\{\vartheta_{sw,SpMax}, \vartheta_{sw,SpH}+\Delta\vartheta_{SpH}\} \tag{24}$$

A similar procedure for the *cooling* mode results in:

$$\vartheta_{sw,SpC,PWM} = \max\{\vartheta_{sw,SpMin}, \vartheta_{sw,SpC}-\Delta\vartheta_{SpC}\} \tag{25}$$

In the *undefined* mode, the supply water temperature set-point range for continuous operation is reduced to $\Delta\vartheta_{sw,SpU,PWM}$. PWM set-points can be calculated with

$$\vartheta_{sw,SpH,PWM} = \vartheta_{sw,SpH} + \frac{R_t}{R_t+\tilde{R}}\cdot\left(\frac{\Delta t_U}{\Delta t_{1,U}}-1\right)\cdot(\vartheta_{sw,SpH}-\vartheta_{r,SpH}) \tag{26}$$

$$\vartheta_{sw,SpC,PWM} = \vartheta_{sw,SpC} - \frac{R_t}{R_t+\tilde{R}}\cdot\left(\frac{\Delta t_U}{\Delta t_{1,U}}-1\right)\cdot(\vartheta_{r,SpC}-\vartheta_{sw,SpC}) \tag{27}$$

where $\Delta t_{1,U}$ is calculated by (22). In all PWM modes, limitations concerning minimal and maximal pump switched-on phases may make it necessary to recalculate the supply water temperature set-points in order to fulfill these limitations (with (26) and (27)).

4.5.2. Purge operation and switch-off criteria

At the beginning of each PWM period, it is recommended to execute a purge operation (a typical minimal purge phase $\Delta t_{1,Purge,Min}$ lasts about 30 min). During this operation, the zone pump is running while the heating and cooling valves are closed: the heating/cooling medium circulates without being heated or cooled. After the initial purge operation $\Delta t_{1,Purge,Min}$, the measured supply water temperature ϑ_{sw} is analyzed:

- If ϑ_{sw} is within the set-point range $[\vartheta_{sw,SpH}, \vartheta_{sw,SpC}]$, the purge phase is prolonged until the switched-on phase is concluded or ϑ_{sw} leaves the range $[\vartheta_{sw,SpH}, \vartheta_{sw,SpC}]$.

- If ϑ_{sw} is outside the set-point range $[\vartheta_{sw,SpH}, \vartheta_{sw,SpC}]$, the purge phase is concluded and active heating or cooling is necessary according to the set-points $\vartheta_{sw,SpH,PWM}$ and $\vartheta_{sw,SpC,PWM}$.

After the conclusion of the initial (minimal) purge phase $\Delta t_{1,Purge,Min}$ and during the remaining switched-on phase, the appropriate switch-off criterion derived from (23) is checked.

Heating mode switch-off criterion:

$$\int_{t=0}^{\Delta t_{1,H}} \vartheta_{sw}(t)dt > \Delta t_{1,H} \cdot \vartheta_{sw,SpH} + \frac{R_t}{R_t + \tilde{R}} \cdot (\vartheta_{sw,SpH} - \vartheta_{r,SpH}) \cdot (\Delta t_H - \Delta t_{1,H}) \quad (28)$$

Cooling mode switch-off criterion:

$$\int_{t=0}^{\Delta t_{1,C}} \vartheta_{sw}(t)dt < \Delta t_{1,C} \cdot \vartheta_{sw,SpC} - \frac{R_t}{R_t + \tilde{R}} \cdot (\vartheta_{r,SpC} - \vartheta_{sw,SpC}) \cdot (\Delta t_C - \Delta t_{1,C}) \quad (29)$$

Undefined mode switch-off criterion:

$$\Delta t_{1,U} \cdot \vartheta_{sw,SpH} + \frac{R_t}{R_t + \tilde{R}} \cdot (\vartheta_{sw,SpH} - \vartheta_{r,SpH}) \cdot (\Delta t_U - \Delta t_{1,U}) < \int_{t=0}^{\Delta t_{1,U}} \vartheta_{sw}(t)dt < \Delta t_{1,U} \cdot \vartheta_{sw,SpC} - \frac{R_t}{R_t + \tilde{R}} \cdot (\vartheta_{r,SpC} - \vartheta_{sw,SpC}) \cdot (\Delta t_U - \Delta t_{1,U}) \quad (30)$$

If ϑ_{sw} is equal to the respective set-point, the switched-on phases are exactly given by (20)–(22), respectively. After the zone pump has been switched off and the rest of the PWM period has run out, the pump is again turned on at the beginning of the next PWM period.

5. Application of PWM control: laboratory tests

The applicability and performance of the presented PWM control methods were assessed by detailed building simulations. In a second step, the simplified PWM control solution was evaluated in laboratory tests performed at the Siemens HVAC-Laboratory in Zug, Switzerland. Some results of these laboratory tests are presented in the following.

5.1. Laboratory test room data

The HVAC-Laboratory test room used is specifically designed to reproduce the thermal behavior of offices in modern commercial buildings equipped with concrete core conditioning and different types of floors and ceilings (Fig. 8). Both floor and ceiling of the test room are equipped with TABS. Special attention has been paid to the test room boundaries. In an assumed office building comprising identical office rooms, there is no heat transfer between adjacent rooms on the same level. Therefore it is sufficient to just insulate these boundaries of the test room well. As there is an inevitable vertical temperature gradient in the room there will be heat transfer from the office room to the adjacent rooms above and below. For this reason these boundaries of the test room can be heated or cooled according to the actual surface temperatures in the test room: In the presented test cases, the ceiling surface temperature was measured and used as set-point for the boundary condition temperature at the lower side of the floor. Analogous, the floor surface temperature was measured and used as set-point for the boundary condition temperature at the upper side of the ceiling. Following such a procedure, rooms above and below are "simulated" that have the same temperature behavior as the test room itself. The thermal influence of the outside temperature on the test room can be simulated by a weather zone built in front of the test room's facade. Characteristics of the test room are summarized in Table 2 and the resulting combined thermal resistances can be found in Table 1.

Table 2
Characteristics of laboratory test room and incorporated TABS.

Room	
Space length, width, height	6 m × 4.2 m × 3.3 m
Façade to weather zone	
Area	14.1 m^2
Overall *U*-value[a]	4.6 W/(m^2 K)
Ventilation	None
TABS configuration	
TABS covering fraction (floor area)	100%
Thickness concrete slab	250 mm
Pipe spacing	150 mm
External/internal pipe diameter	20/15 mm
Specific mass flow rate[b]	15 kg/(h m^2)
Thermal resistance of floor coverage (raised floor, carpet)	0.5 (m^2 K)/W
Thermal resistance of ceiling coverage (bare)	0 (m^2 K)/W

[a] In order to be able to "simulate" a large outside temperature range, an unrealistically high *U*-value for the façade has been chosen.
[b] In terms of floor area covered by TABS.

5.2. Applied heat gains and control parameters

In the laboratory test room, heat gains were brought in exclusively by heat dissipation devices (cooling load simulators, see

Fig. 8. HVAC-Laboratory test room equipped with TABS: external view from the laboratory hall (left) and view from the weather zone into the room (right).

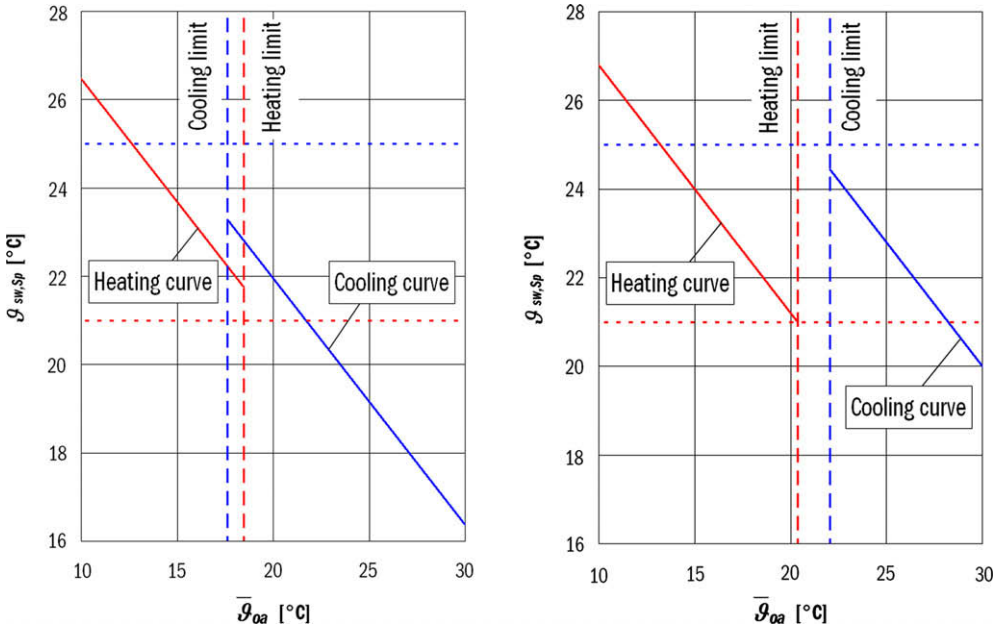

Fig. 9. Heating/cooling curves and heating/cooling limits for test scenarios workdays (left) and weekend (right); here $\overline{\vartheta}_{oa}$ represents the mean weather zone temperature of the last 24 h).

Fig. 8 right). A repeating weekly sequence of heat gains was applied to reflect the daily heat gain inputs in a typical office room, differentiating between 5 workdays (maximal gains 20–30 W/m^2) and 2 weekend days (maximal gains 3–5 W/m^2), cf. Fig. 10.

For both the workday and the weekend situation, an integrated design procedure as introduced in [10,11] was carried out. This at first led to the equivalent heat gain bounds (see Table 1 for equivalent heat gains of workdays), and finally to the heating and cooling curves and limits shown in Fig. 9.

5.3. Test results

In Table 3, conditions and parameter values for two test cases are given. In the first test case, we considered a PWM in *cooling* mode with a PWM period of 24 h. The beginning of each switched-on phase was set to be at 10 pm. Such a setting is energy efficient when outside air temperatures are significantly lower during the night and cooling is provided by a cooling tower. In the second test case, a PWM in *heating* mode with a PWM period of 5 h was considered.

The choice of the PWM period is a trade-off between slightly worse room temperature control for long switched-off phases (occurring when using long PWM periods) and a higher number of (unproductive) purge phases with short PWM periods. For typical concrete core-activated structures and PWM periods up to 24 h, resulting room temperature amplitudes from PWM are small and the defined comfort criteria (comfort band) can be met independently of the chosen PWM period. In addition, with PWM periods of 24 h, it is possible to place switched-on phases to a given time of day interval and benefit from higher energy efficiency or lower energy costs.

Room temperatures shown in the result figures (Figs. 10 and 11) are measured operative temperatures in the middle of the room at 1.2 m height.

Fig. 10 shows test results for case 1. During the first 3 days and the last day shown, large heat gain inputs were present from 8 am to 6 pm (workday situation); during day 4 and 5 there were only low heat gains (weekend situation). At the beginning of each PWM switched-on phase, a purge phase was initiated. The initial purge phase was succeeded by a cooling phase (see Fig. 10, pump axis, marked by pale areas) in the workday situation or was prolonged in the weekend situation. Note that when the pump is switched off, supply and return temperature measurements are not meaningful for control.

Fig. 11 shows test results for case 2. During the first 2 days and the last 2 days shown, large heat gain inputs were present from 8 am to 6 pm (workday situation); during day 3 and 4 there were only low heat gains (weekend situation). At the beginning of each PWM switched-on phase, a purge phase was initiated. Here, the initial purge phase was prolonged for all but six switched-on phases in which heating activities were necessary (see Fig. 11, pump axis, marked by pale areas).

Table 3
Conditions and parameter values for the laboratory test cases.

Parameter	Case 1	Case 2
Weather zone temperature ϑ_{oa}	22 °C	15 °C
Lower room temperature set-point $\vartheta_{r,SpH}$	21 °C	21 °C
Upper room temperature set-point $\vartheta_{r,SpC}$	25 °C	25 °C
PWM period Δt	24 h	5 h
PWM set-point shift $\Delta\vartheta_{SpH}$	1.5 K	1.5 K
PWM set-point shift $\Delta\vartheta_{SpC}$	1.5 K	1.5 K
PWM minimal purge phase $\Delta t_{1,Purge,Min}$	30 Min	30 Min
PWM switched-on phase start time	10 pm	–
Room temperature feedback control	Disabled	Enabled

6. Conclusions and outlook

The presented PWM control method for thermally activated building systems (TABS) is one module of a new control concept that is one part of an integrated process consisting of TABS design (planning of HVAC system and its control), commissioning of TABS and optimization during operation. Such an integrated process enhances the reliability of the design and the operation and alleviates the effort for control parameter tuning. PWM control operates the TABS zone pump in an intermittent way which allows for energy efficient control solutions: Energy consumption for transportation of the heating/cooling medium can be reduced, and the PWM

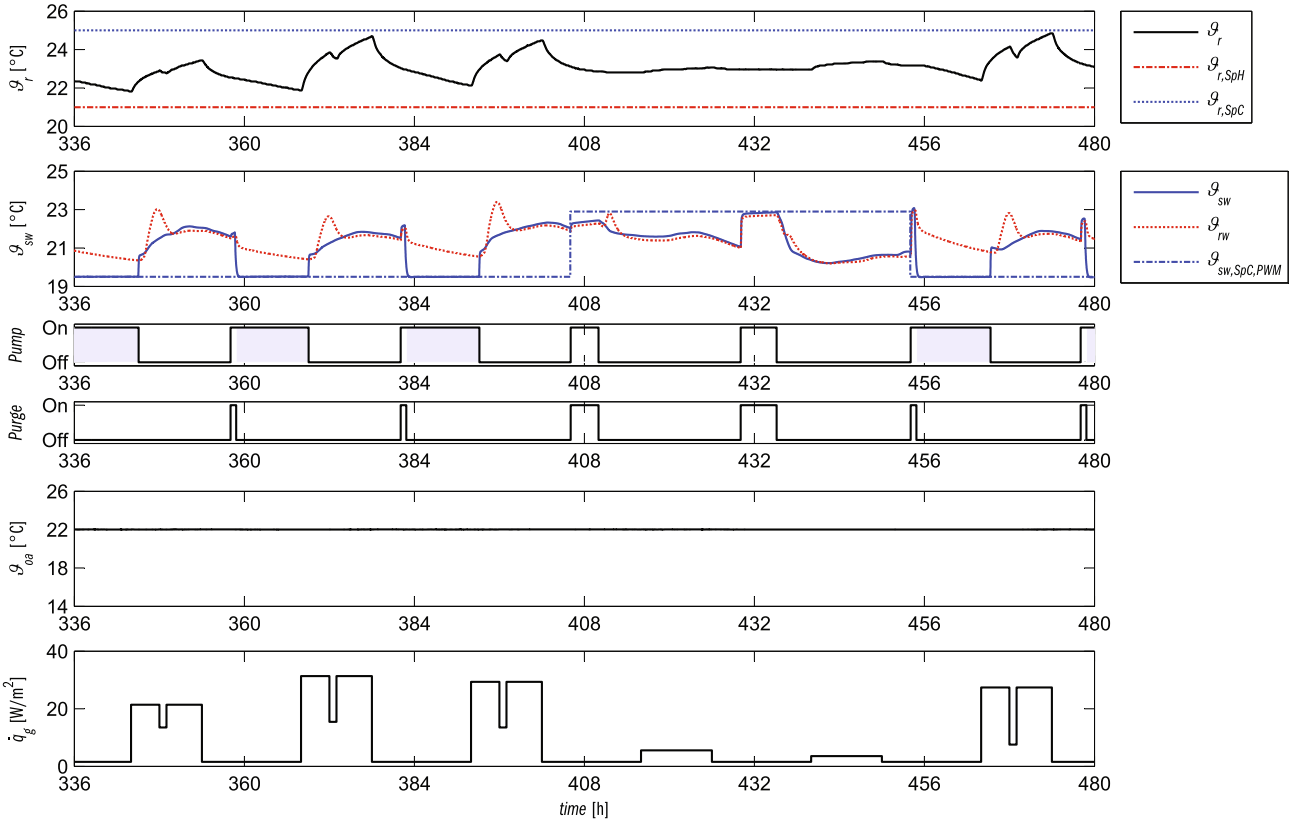

Fig. 10. PWM control test results for cooling mode with $\Delta t_C = 24$ h (case 1).

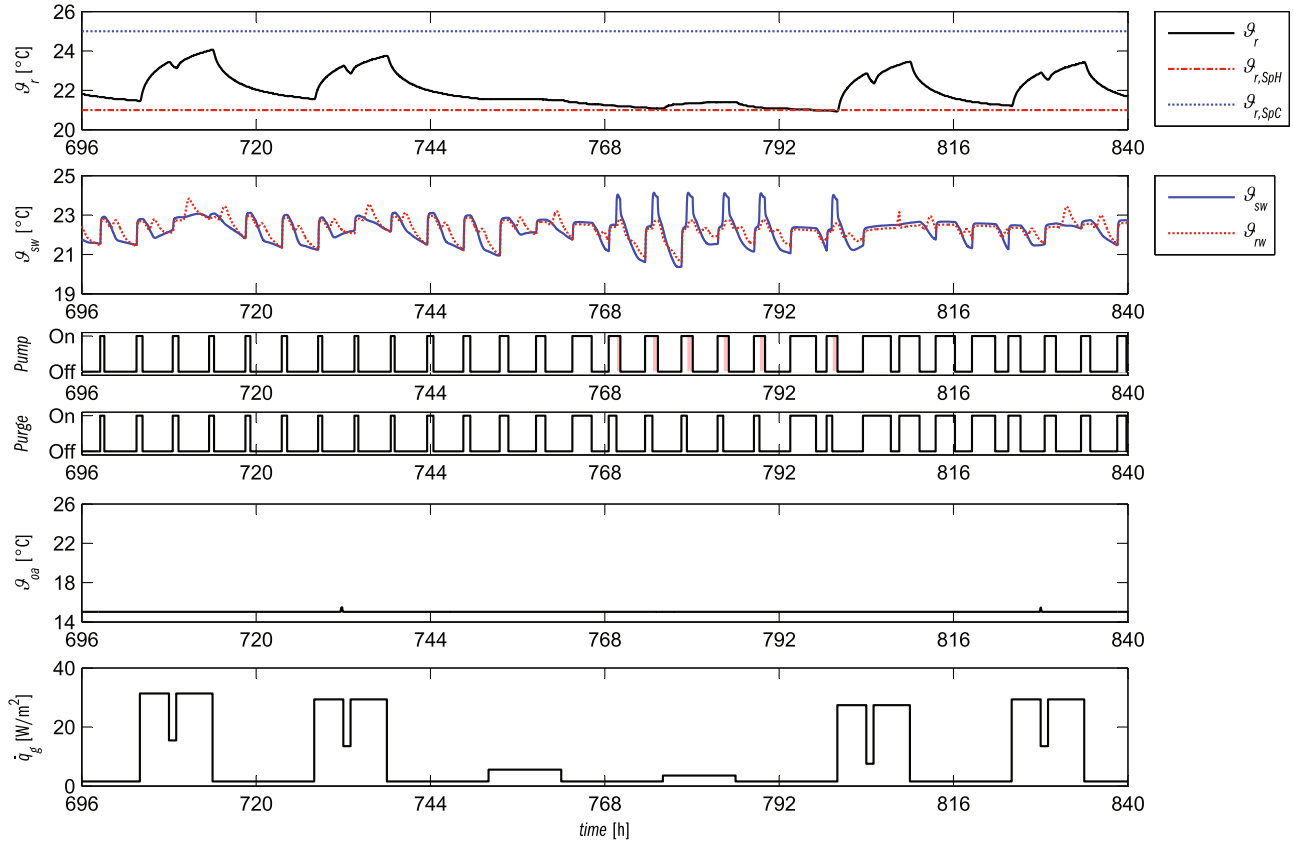

Fig. 11. PWM control test results for heating mode with $\Delta t_H = 5$ h (case 2).

switched-on phases can be shifted to times with high energy generation efficiency (e.g. benefit from colder night time outdoor temperatures). The quantification of energy reduction potentials using PWM control is a topic of ongoing and future investigations.

Two PWM control solutions are outlined and compared in this paper, one based on a 1st order thermal model of a room equipped with TABS, and a simplified PWM control solution. Simulation studies [12] show that both solutions are sufficiently accurate for application in building control, the simplified solution having the advantage of only one control parameter to tune. That simplified solution was additionally evaluated in tests performed at the Siemens HVAC-Laboratory in Zug, Switzerland. For two of the test cases carried out, results are shown and analyzed in the paper. In the laboratory test set-up, it has been confirmed that the simplified PWM control solution successfully works for all assessed test cases. The PWM control module has proved to fit well into the newly developed TABS control solution. Furthermore, the module is easy to engineer and commission which qualifies it for practical application.

Further details of the PWM method and the entire newly developed TABS control solution can be found in the design and commissioning handbook, published in the frame of our work [12].

Acknowledgements

The partial funding of the project by the Swiss Confederation's innovation promotion agency CTI and the input of the project steering committee are gratefully acknowledged.

References

[1] Koschenz M, Dorer V. Interaction of an air system with concrete core conditioning. Energy Build 1999;30(2):139–45.
[2] Lehmann B, Dorer V, Koschenz M. Application range of thermally activated building systems TABS. Energy Build 2007;39(5):593–8.
[3] Koschenz M, Lehmann B. Thermoaktive Bauteilsysteme TABS. Duebendorf (Switzerland): Empa; 2000. ISBN 3-905594-19-6 [in German].
[4] Güntensperger W, Gwerder M, Haas A, Lehmann B, Renggli F, Tödtli J. Control of concrete core conditioning systems. In: Proceedings: 8th REHVA world congress Clima 2005, Lausanne (Switzerland).
[5] Gwerder M, Lehman B, Tödtli J, Dorer V, Renggli F. Control of thermally activated building systems TABS. Appl Energy 2008;85(7):565–81.
[6] Meierhans R. Room air conditioning by means of overnight cooling of the concrete ceiling. ASHRAE Trans 1996;102(1):693–7.
[7] Olesen BW. Radiant floor heating in theory and practice. ASHRAE J 2002:19–26.
[8] Antonopoulos KA, Vrachopoulos M, Tzivanidis C. Experimental and theoretical studies of space cooling using ceiling-embedded piping. Appl Therm Eng 1997;17(4):351–67.
[9] Weitzmann P. Modelling building integrated heating and cooling systems. PhD thesis. Danish Techn University. Rapport BYG·DTU R-091 2004; ISBN 87-7877-155-2; 2004.
[10] Gwerder M, Tödtli J, Lehman B, Renggli F, Dorer V. Control of thermally activated building systems. In: Proceedings: 9th REHVA world congress Clima 2007, Helsinki (Finland).
[11] Tödtli J, Gwerder M, Lehman B, Renggli F, Dorer V. Integrated design of thermally activated building systems and of their control. In: Proceedings: 9th REHVA world congress Clima 2007, Helsinki (Finland).
[12] Tödtli J, Gwerder M, Lehmann B, Renggli F, Dorer V. TABS-Control: Steuerung und Regelung von thermoaktiven Bauteilsystemen. Faktor Verlag Zurich (Switzerland); 2009. ISBN: 978-3-905711-05-9 [in German].
[13] Standard EN 15377-1. Heating systems in buildings – design of embedded water based surface heating and cooling systems – part 1: determination of the design heating and cooling capacity; 2008.
[14] Tödtli J. Influence of thermal inertia on heating controller adaptation: an analytical investigation. In: Proceedings: 3rd REHVA world congress Clima 2000 (1993), London (England).